Correlation between seismic intensity for the Maule 2010 earthquake (Mw 8.8) and microtremors' HVSR

F. Leyton
Universidad Diego Portales, Chile

S. Ruiz & M. Astroza
Universidad de Chile, Chile

SUMMARY: (10 pt)
The Maule 2010 earthquake (Mw 8.8) had a very large rupture, with strong shaking that affected many cities located in different soil conditions. Nearly 100 cities located at or near the epicentral zone were surveyed and MSK seismic intensity reported (Imsk). In the present study, we performed microtremors' measurements at these localities and computed the horizontal-to-vertical spectral ratio (HVSR). We found a strong correlation between increments/decrements of the seismic intensity and the microtremors' HVSR response. For example, for those localities that presented larger seismic intensities, we found HVSR curves with a clear peak, with frequencies ranging from 0.3 up to 5.0 Hz. On the other hand, those localities with decrements in seismic intensities are mostly characterized by either flat HVSR curves (without a clear predominant frequency) or predominant frequencies above 5.0 Hz. These results support the use of microtremors' HVSR as an effective technique for microzonation purposes.

Keywords: microtremors' HVSR, MSK seismic intensity, Maule 2010 earthquake, Central Chile

1. INTRODUCTION

The 2010 Maule earthquake is one of the largest earthquake since modern recording began, and the largest in Chile after the 1960 Valdivia earthquake (Mw 9.5). The earthquake occurred on a locked megathrust fault resulting from oblique convergence of the oceanic Nazca plate subducting beneath the continental South American plate at ~ 6.5 cm/yr (Kendrick et al., 2003); the subduction segment located between 35°S and 37°S had been shown to be strongly coupled (Ruegg et al., 2009; Madariaga et al., 2010) with a large slip deficit accumulated since the 1835 earthquake. The aftershock distribution indicates that the event filled a seismic gap along the 1835 earthquake rupture zone, and that the rupture also extended well to the north, spanning regions that ruptured in 1928, 1985 and about 2/3 of the 1906 rupture zone (Beck et al., 1998). Several studies have been devoted to the analysis of the source process of this event (e.g. Lay et al., 2010; Delouis et al., 2010; Tong et al., 2011; Ruiz et al., 2011) giving an improved understanding of this large earthquake. However, very few studies have been focused on the damaged produced by this event (Astroza et al, 2010, 2012; Ruiz and Astroza, 2012; Ruiz et al, 2012). Astroza et al. (2012) showed that, from 111 localities, only 8 of them exceeded MSK intensity (Imsk) VIII and 79% were below VII (see Fig. 1.1). This Figure presents the Imsk reported by Astroza et al. (2012), obtained by field surveys few days after the Maule 2010 earthquake; we numbered the 8 localities with Imsk ≥ VIII, marked with a black star in Fig. 1.1. We also present the isoseismal curves drawn by these authors, considered for locations over hard soil (compact and old alluvial or fluvial deposits) as considered by Astroza et al. (2012). In the same Figure, we plot the finite-fault slip distributions obtained by inversion of teleseismic P waves, SH waves, and R1 STFs (taken from Fig 3 of Lay et al., 2010). Considering slip distribution observed from this event, Ruiz et al. (2012) concluded that the damage observed was controlled mainly by the northern asperity, the one that presented the higher slip.

Microtremors have been extensively used in the prediction of increments in damage produced by large earthquake or seismic site effects (Bard, 1990; Lermo and Chávez-García, 1993; Chávez-García et al., 2007; Leyton and Ruiz, 2011). One of the most used techniques, due to its economy and simplicity, is the horizontal-to-vertical spectral ratio (HVSR), known as Nakamura's technique (Nakamura, 1989; 2000), usually used in the estimation of the predominant vibration frequency of the soil (Lermo y Chávez-García, 1993; 1994; Lachet et al., 1996; Konno and Ohmachi, 1998; Bonnefoy-Claudet et al., 2006a; 2006b; 2008b). This method has been previously applied in Chile to study Santiago and Valparaíso (Pasten, 2007; Bonnefoy-Claudet et al., 2009; Pilz et al., 2009; Leyton et al., 2011) showing that, in most cases, the predominant frequency of the soil can be successfully estimated.

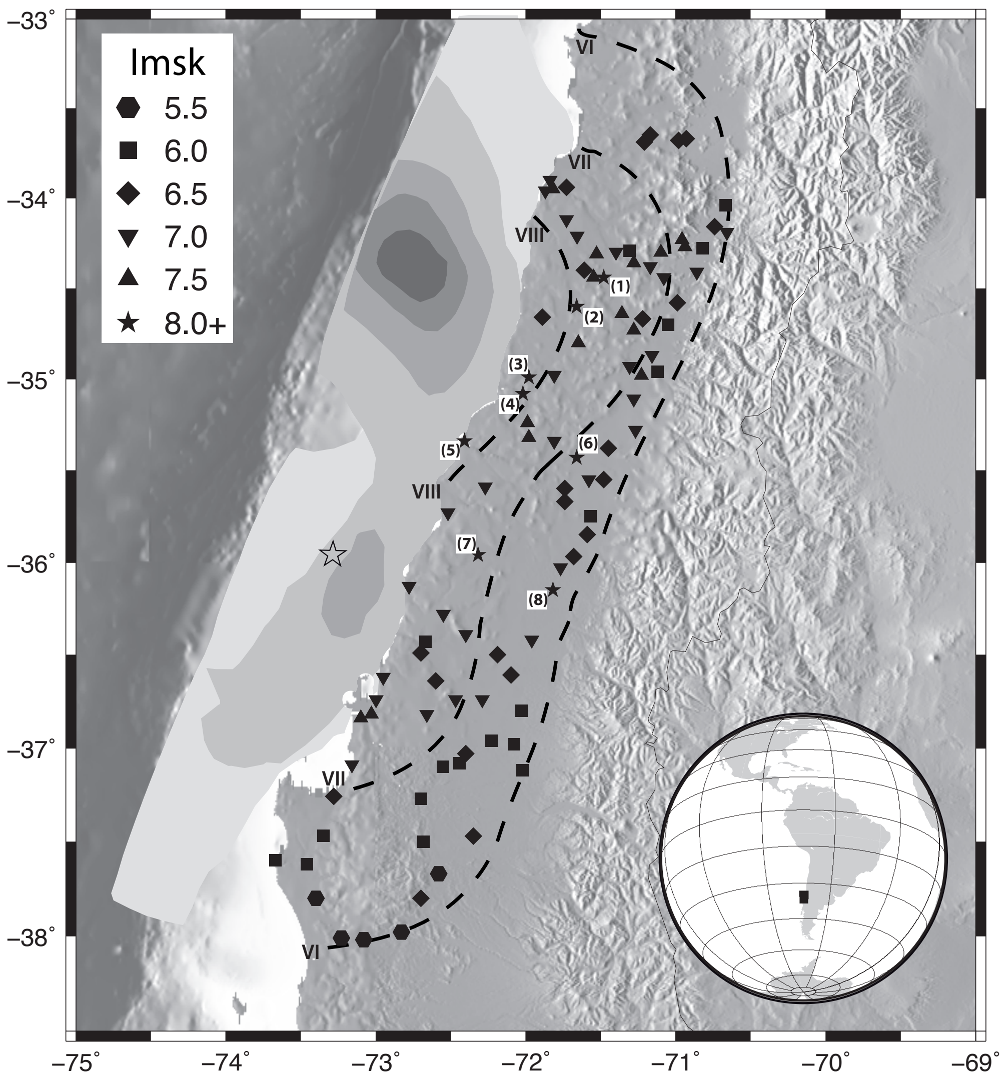

Figure 1.1. Topographic map with MSK seismic intensities (Imsk) shown in symbols (see scale on the upper right corner) reported for the Maule 2010 earthquake by Astroza et al. (2012); the dashed lines represent the isoseismals at hard soil conditions. The numbers show the localities with Imsk greater or equal to VIII. We also show the finite-fault slip distributions obtained by Lay et al. (2010), see text for details. The insert in the lower right shows the location of the study area.

In the present study, we show the results from more than 600 3-component, single station, microtremors measurements at 99 localities with reported MSK seismic intensity (Imsk) of the Maule 2010 (Mw 8,8) earthquake. We found that localities with Imsk ≥ VIII present a clear peak in microtremors' HVSR, with amplitudes above 2, having a clear predominant frequency; these frequencies range from 0.3 up to 5.0 Hz. Considering this feature, we classify all the microtremors' HVSR curves as predicting the existence of site effect or the lack of it, and compared these predictions with the observed increase/decrease of Imsk with respect to hard soil sites. From all the localities, 61% of them we were able to predict the presence/absence of site effect; while only for 2 sites had no prediction of site effect amplification and an increment of the observed MSK seismic intensity. Hence, we conclude that microtremors' HVSR are an effective and inexpensive method to estimate an increase in the damage produced by large earthquakes.

2. METHODOLOGY

In this study, we used a 3-component 4.5-Hz GVB instrument to make each one of the measurements, which gives a reliable answer down to 0.1 Hz and has been successfully used in this kind of studies (Leyton et al., 2011; Leyton and Ruiz, 2011). At each point, we recorded for a time window of at least 15 min, depending on the level of human activity, as recommended for microzonation studies (Bard and SESAME Workgroup WP02, 2005). Later, we processed each data in the same way: we divided the total time window into 60-sec subwindows, giving reliable results down to 0.05 Hz. Then, we computed the S-transform of each component (Stockwell et al., 1996) and added the modulus of both horizontals creating a composed horizontal that assumes perfect coherency between them. Note that this last quantity is the largest possible estimator of the power observed at the horizontal components. Later on, we smoothed the composed horizontal and vertical components with a homogenous filter in log-scale (Konno and Ohmachi, 1998), enabling the computation of the horizontal over vertical spectral ratio. Due to the fact that we used the S-transform, we get an estimation of the Fourier Spectrum at each point that we average with all the other 60-sec subwindows; resulting in a smooth version of the horizontal energy over the vertical. A couple of examples are shown in Fig. 2.1, as discussed in detail in the following paragraph. Note that the S-transform has been successfully applied in detailed analysis of time series (e.g. Pinnegar et al., 2003; Parolai, 2009).

In order to see if the estimation of the predominant frequency was biased by noise, we plotted the HVSR of each 60-sec subwindow and compared the result of the average. Fig. 2.1 shows the results for 2 cases: to the left (from (a) to (c)) is a case with a clear predominant frequency at 2.0 Hz, while at the right ((d) to (f)) is a case considered a flat HVSR curve, with no clear predominant frequency. The lower panels, (c) and (f), show the geometric average HVSR (continuous line) and the corresponding standard deviation (gray area), the usual representation of these kinds of results. We also plotted the geometric average of the HVSR for each subwindow, as shown in panels of (b) and (e); the shade of gray is proportional to the spectral ratio, following the scale at the middle. From these panels, a clear predominant frequency will be marked by dark shades of gray, as in case (a) at 2.0 Hz; while panel (d) shown no predominant frequency in any subwindow. Panels (b) and (e) present the number of subwindows that exceeds the corresponding HVSR value, following the scale at the right. Following this, black represents the value where half of the windows have an HVSR lower or equal, while the other half being higher, representing the statistical mode. In general, there is an agreement between the mode and geometric average; unless there are few measurements that increase the average. This could be the case due to the fact that we are averaging values where the denominator can decrease, dramatically increasing the ratio. Panel (b) shows agreement with panel (c), meaning a reliable estimation of the representing HVSR curve; while panel (d) shows no clear peak, in contrast with panel (f) that shows a peak at lower frequencies, this is explained by few subwindows with extremely large values at low frequencies that do not represent the actual HVSR. Hence, we conclude that the measurement on the left has a clear predominant frequency at 2.0 Hz; while the second measurement have a flat HVSR curve, with no predominant frequency. We processed each measurement in the same way, in order to make robust estimations of the predominant frequency, or the absence of it.

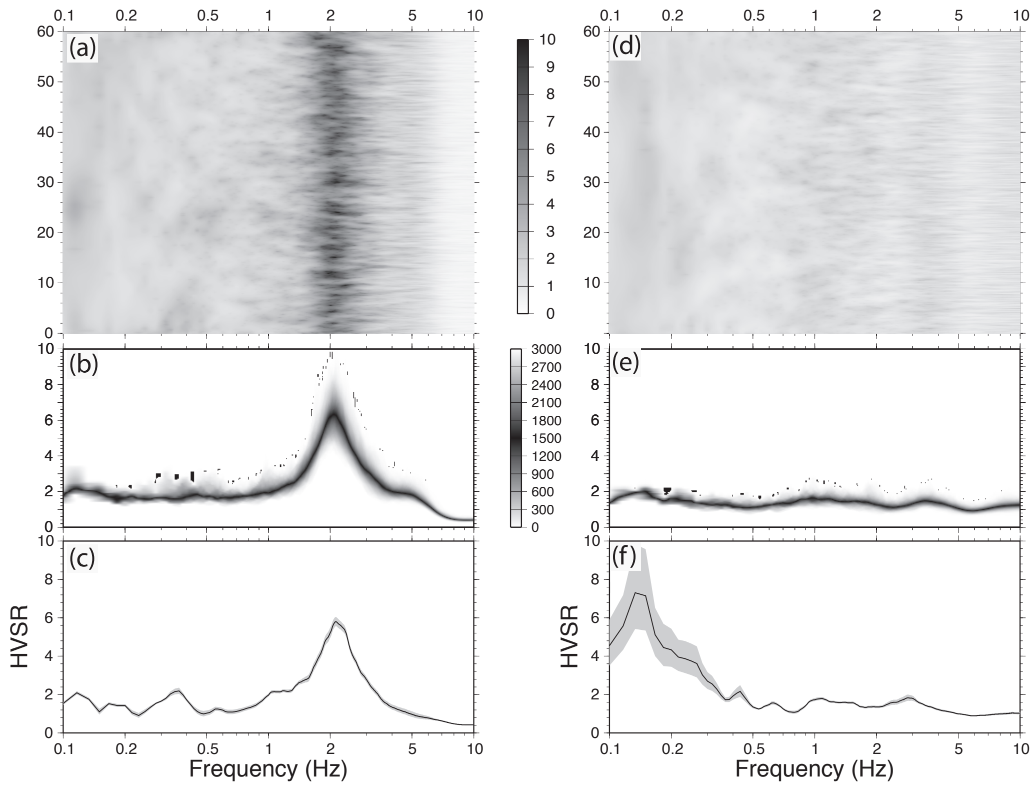

Figure 2.1. Examples of microtremors' horizontal-to-vertical spectral ratio (HVSR). Lower panels ((c) and (f)) show the average HVSR (continuous line) and the standard deviation in log-scale (gray area). Middle panels ((b) and (d)) show the number of subwindows exceeding the corresponding HVSR value, following the scale on the middle; hence, black here represents the statistical mode. Top panels ((a) and (c)) show the HVSR for each subwindow, being the shade of gray proportional to HVSR following the scale on the middle.

Previous studies have shown that the presence of large a amplitude peak is related to a high impedance contrast between the sedimentary cover and the basement, while a low amplitude peak is related to a lower contrast, indicating the presence of a hard soil (Woolery and Street, 2002; Bonnefoy-Claudet et al, 2006a; 2008b). In cases with a large peak on the HVSR curve, we have a good estimator of the predominant frequency of the soil (Tokimatsu, 1997; Bonnefoy-Claudet et al., 2006a; 2008b).

3. RESULTS

We found that in all localities with MSK seismic intensity equal or larger than VIII, there is a clear peak in microtremors' HVSR with amplitudes larger than 2, as shown in Fig. 3.1. This can be considered as a clear indication of a predominant frequency at those places, ranging from 0.3 up to 5.0 Hz (see Fig. 3.1). From Fig. 1.1 we see that the 8 localities have different locations, with only 3 of them inside the isoseismal VIII: (3) Licantén, (4) Curepto, and (5) Constitución, 3 within isoseismal VII: (1) Peralillo, (2) Pumanque, and (7) Cauquenes, and 2 sites within isoseismal VI: (6) Talca and (8) Parral. Therefore, the extensive damage observed at these sites cannot be explained by the distance to the source, to the fault plane or to the main asperities, but rather by the effects of local conditions; we use this criterion to define the possibility of having seismic amplifications at a specific site.

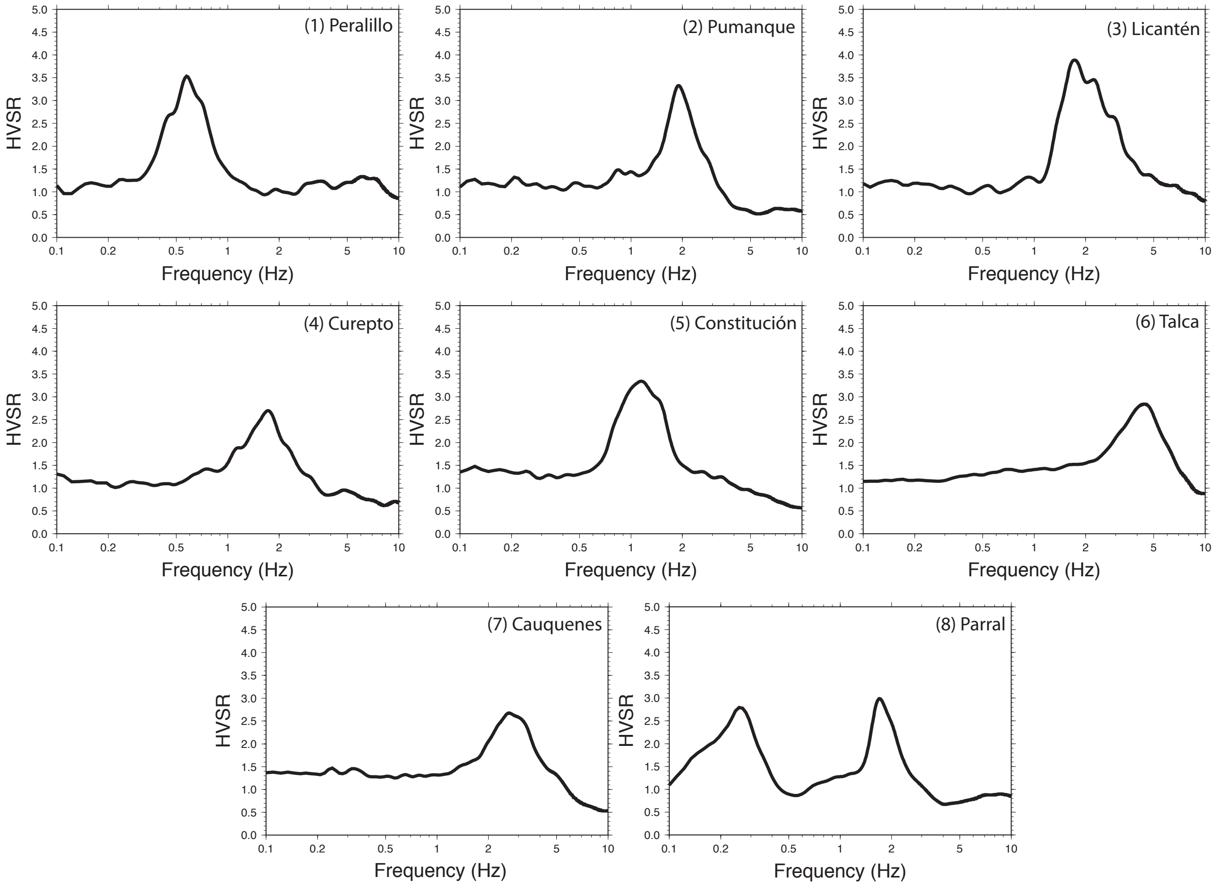

Figure 3.1. Average response of microtremors' horizontal-to-vertical spectral ratio (HVSR) for localities with MSK seismic intensity equal or greater than VIII. The location of each site is shown with numbers in Fig. 1.1. Note that all curves have a clear peak (above 2), marking a predominant frequency between 0.3 and 5.0 Hz.

As mentioned before, we performed at least 5 15-min measurements at each locality, making more of them at larger cities. In order to estimate 1 single behavior for each locality, we combined all the measurements in a single estimation. We followed Tichelarr and Ruff (1989) to make a robust estimation of the predominant frequency using bootstrapping. From a pool that included all 1-min windows, we selected a subset of 90% of the total, without repetition. Then, from that subset, we estimated the predominant frequency by computing the geometrical average. We repeated this procedure for 100 times and obtained the same number estimations of the predominant frequency, enabling the robust estimation of it. We defined that a locality presented site effect if a predominant frequency was found (with and HVSR amplitude larger than 2) between 0.3 and 5.0 Hz. For those places with predominant frequencies above 5.0 Hz or HVSR amplitudes lower than 2, we considered that no site effect should be observed. The results are presented in Fig. 3.2, having a circle around those localities that we think should have seismic amplifications; from all the sites studied, 66% presented conditions for site effect.

Fig. 3.2 also shows the increase/decrease of MSK seismic intensity (ΔImsk) with respect to the isoseismals; recall that these curves were drawn considering sites with hard soils conditions (Astroza et al., 2012). These decrements/increments are shown in discrete shades of blue/red, with white representing those localities with no or negible ΔImsk, in other words, those localities without significant site effect. This Figure shows in black stars the localities with Imsk ≥ VIII; remember that the characteristics presented by these sites are the ones that define the possibility of site effect: a clear peak in HVSR curve (above 2), with predominant frequency between 0.3 and 5.0 Hz.

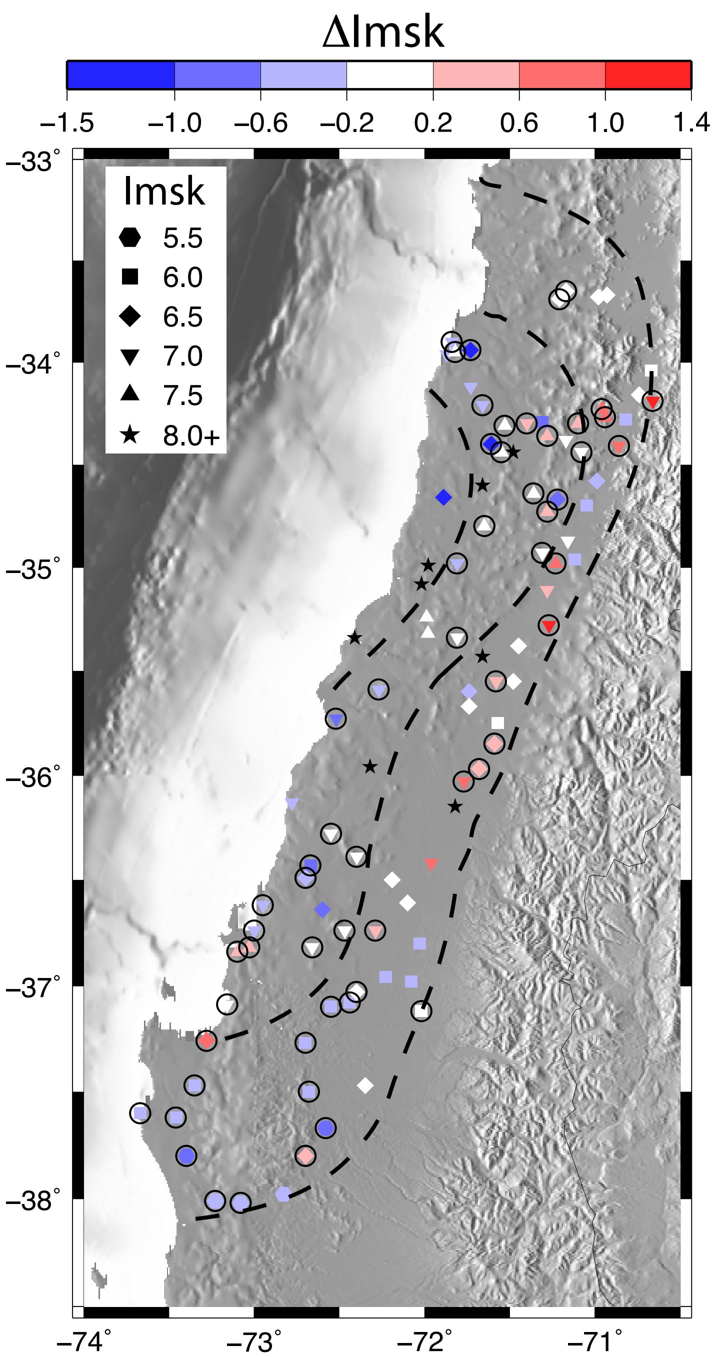

Figure 3.2. Topographic map with MSK seismic intensities (Imsk) shown in symbols (see scale on the upper right corner) reported for the Maule 2010 earthquake by Astroza et al. (2012); the dashed lines represent the isoseismals at hard soil conditions. The colors are proportional to Imsk deamplification (shades of blue) or amplification (shades of red); while the circles surrounding a symbol represent the prediction of site effect (see text for details).

From Fig. 3.2 we can see that there are some localities that present a clear peak in the microtremors' HVSR curve (above 2), with predominant frequencies between 0.3 and 5.0 Hz; we considered these site to have a "Predicted Site Effect" and are marked with circles in this Figure. Also, we can see that some localities have clear increments of Imsk, shown in shades of red in Fig. 3.2; while other present clear decrements of Imsk, shown in shades of blue in Fig. 3.2. All these combinations can be grouped into 6 cases, as presented in Table 3.1 from (i) up to (vi). Note that the 8 sites that presented Imsk ≥ VIII are classified into case (i) with Predicted Site Effect and positive increment of seismic intensity (ΔImsk increase).

Table 3.1. Data For Beams Under Dynamic Loading (10 pt regular)

Case	Predicted Site Effect	ΔImsk	Total
(i)	Yes	Increase	28
(ii)	No	Decrease	17
(iii)	No	No change	15
(iv)	Yes	No change	16
(v)	Yes	Decrease	21
(vi)	No	Increase	2

From Table 3.1, we can see that 61% of the observations follow the behavior predicted from microtremors' HVSR by either having a predicted site effect and increments of Imsk (28%, case (i)) or no predicted site effect with decrease or no change in the MSK seismic intensity (32%, cases (ii) and (iii), respectively) with respect to hard soil conditions. On the other hand, 37% of the observations have a predicted site effect but show no increments in Imsk, or even some decrements (cases (iv) and (v), respectively). Finally, only 2% of the observations present a clear increment in seismic intensity, but were not predicted to have site effect (case (vi)), being the worst-case scenario. Note that 22 of the 39 observations, 56% of cases (iv) and (v), are located southern of 36ºS, mostly affected by the southern asperity, the one with lower slip on the fault (see Fig. 1.1). This might offer an explanation of the absence in increment of MSK seismic intensity (either by no increase or decrease of ΔImsk) by the lack of seismic energy to trigger site effect conditions; nevertheless, this issue should be further investigated to be able to reach to any conclusion.

5. CONCLUDING REMARKS

In this study we present the results from more than 600 3-component, microtremors measurements at almost 100 localities with reported MSK seismic intensity (Imsk) for the Maule 2010 earthquake. From these measurements, we computed the horizontal-to-vertical spectral ratio (HVSR) and correlated with the reported Imsk. We found that, for those localities with Imsk equal or larger than VIII (8 in total), the HVSR presented a clear peak, with amplitude above 2, showing a predominant frequency between 0.3 and 5.0 Hz. Using this characteristics as a prediction of site effect, we studied the other 91 localities.

Therefore, for those site with a clear peak in the HVSR curve (above 2) and a predominant frequency between 0.3 and 5.0 Hz, we assume that there should be conditions for amplification of the damage produced by a large earthquake, without any other source of information (such as surface geology, description of the shear wave velocity in the upper meters, etc.). From the 99 localities studied, 66% presented conditions of site effect while the remaining 34% showed no clear peak in the HVSR curve (below 2) or a predominant frequency over 5.0 Hz.

Comparing the prediction of site effect with the observed increments/decrements of MSK seismic intensity (ΔImsk) we found that in 61% of the cases we were able to predict the site effect. From those sites with unsuccessful prediction, a 56% of the cases are located below the 36ºS, closer to the southern asperity that was shown to released lower slip over the fault (see, for example Lay et al., 2010; or Delouis et al. 2010). We believe that the lack of site effect observed in those localities is due to the lack of seismic energy released at high frequencies; nevertheless, this issue should be further studied.

It's worth noting that only 2 cases we observed an increment in seismic intensity (ΔImsk > 0) with no prediction of site effect, both of them presented Imks = VII in an area where and intensity VI-VII should be expected. These exceptions should be explored further in order to explain this amplification maybe due to surface geology.

Finally, we believe that, even though in 37% we expected seismic amplifications and none could be observed or deamplification was found, the use of 3-component, microtremors HVSR are an economical and efficient method to predict the possibility of having site effect, with no other information available. This encourages the use of this technique for seismic microzonation purposes.

AKCNOWLEDGEMENTS

This work was financed by Fondecyt 1100551 and Milleniun Nucleus on Seimotectonics and Seismic Hazard. The figures were made using GMT (Wessel and Smith, 1991).

REFERENCES

Astroza, M., Ruiz, S., Astroza, R. (2012) Damage assessment and seismic intensity analysis of the 2010 (Mw 8.8) Maule earthquake. *Earth. Spectra*. Submitted.

Astroza, M., Cabezas, F., Moroni, M.O., Massone, L., Ruiz, S., Parra, E., Cordero, F. and Mottadelli, S. (2010) Intensidades sísmicas en el área de daños del terremoto del 27 de febrero de 2010, Departamento de Ingeniería Civil, Facultad de Ciencias Físicas y Matemáticas; Universidad de Chile, Santiago, Chile.

Bard, P. Y. (1999) Microtremors measurements: a tool for site effect estimation?, *The effects of surface geology on seismic motion,* **3**, 1251-1279.

Bard, P. Y., and SESAME-Team (2005) Guidelines for the implementation for the H/V spectral ratio technique on ambient vibrations-measurements, processing and interpretations, in *SESAME European research project EVG1-CT-2000-00026, deliverable D23.12*, edited, available at http://sesame-fp5.obs.ujf-grenoble.fr.

Beck, S., S. Barientos, E. Kausel, and M. Reyes (1998) Source characteristics of historic earthquake along the central Chile subduction zone, *J. South Am. Earth Sci*., **11**, 115–129, doi:10.1016/S0895-9811(98) 00005-4.

Bonnefoy-Claudet, S., C. Cornou, P. Y. Bard, F. Cotton, P. Moczo, J. Kristek, and D. Fäh (2006a) H/V ratio: a tool for site effects evaluation. Results from 1-D noise simulations, *Geophys. J. Int.* **167**, 827-837.

Bonnefoy-Claudet, S., C. Cornou, and P. Y. Bard (2006b) The nature of noise wavefield and its application for sites studies. A literature review", *Earth Sci.-Rev.* **98**, 288-300.

Bonnefoy-Claudet, S., S. Baize, L. F. Bonilla, C. Berge-Thierry, C. Pasten, J. Campos, P. Volant, and R. Verdugo (2008a) Site effect evaluation in the basin of Santiago de Chile using ambient noise measurements, *Geophys. J. Int.* **176:3**, 925-937.

Bonnefoy-Claudet, S., A. Köhler, C. Cornou, M. Wathelet, and P. Y. Bard (2008b) Effects of Love waves on microtremor H/V ratio, *Bull. Seism. Soc. Am.*, **98:1**, 288-300.

Chávez-García, F. J., T. Dominguez, M. Rodriguez, and F. Pérez (2007) Site effects in a volcanic environment: a comparison between HVSR and array techniques at Colima, Mexico, *Bull. Seism. Soc. Am.* **97**, 591-604.

Delouis, B., Nocquet, J.M., and Vallée, M. (2010) Slip distribution of the February 27, 2010 Mw = 8.8 Maule Earthquake, central Chile, from static and high-rate GPS, InSAR and Broadband teleseismic data. *Geophys. Res. Lett*. **37**, L17305, doi:10.1029/2010GL043899.

Kendrick, E., et al. (2003) The Nazca–South America Euler vector and its rate of change, *J. So. Am. Earth Sci*., **16:2**, 125-131.

Konno, K., and T. Ohmachi (1998) Ground-motion characteristics estimated from spectral ratio between horizontal and vertical components of microtremor, *Bull. Seism. Soc. Am.* **88:1**, 228-241.

Lay, T., C. J. Ammon, H. Kanamori, K. D. Koper, O. Sufri, and A. R. Hutko (2010) Teleseismic inversion for rupture process of the 27 February 2010 Chile (Mw 8.8) earthquake. *Geophys. Res. Lett*. **37**, L13301, doi:10.1029/2010GL043379.

Lachet, C., D. Hatzfeld, P. Y. Bard, N. Theodulidis, C. Papaioannou, and A. Savvaidis (1996) Site effects and microzonation in the city of Thessaloniki (Greece) comparison of different approaches, *Bull. Seism. Soc. Am.* **86:6**, 1692-1703.

Lermo, J., and F. J. Chávez-García (1993) Site effect evaluation using spectral ratios with only one station, *Bull. Seism. Soc. Am.* **83**, 1574-1594.

Leyton, F., and S. Ruiz (2011) Comparison of the behavior of site from strong motion data of the 1985 Central Chile earthquake (Ms=7.8) and microtremors measurements, *5th International Conference on Earthquake Geotechnical Engineering*.

Leyton, F., S.A. Sepúlveda, M. Astroza, S. Rebolledo, P. Acevedo, S. Ruiz, L. Gonzalez, and C. Foncea (2011) Seismic Zonation of the Santiago Basin, Chile, *5th International Conference on Earthquake Geotechnical Engineering*.

Madariaga, R., C. Vigny, M. Métois, and J. Campos (2010) Central Chile finally breaks. *Science* **328**, 181–182, doi:10.1126/science.1189197.

Ruegg, J.C., Rudloff, A., Vigny, C., Madariaga, R., Dechabalier, J.B., Campos, J., Kausel, E., Barrientos, S., Dimitrov, D. (2009) Interseismic strain accumulation measured by GPS in south central Chile seismic gap. *Phys. Earth Planet. Int*., **175**, 78- 85.

Nakamura, Y. (1989) A method for dynamic characteristics estimations of subsurface using microtremors on the ground surface. *Q. Rep. Railway Tech. Res. Inst. Japan,* **30**, 25-33.

Nakamura, Y. (2000) Clear identification of Nakamura's technique and its application. *12th World Conference on Earthquake Engineering*.

Parolai, S. (2009). Denoising of Seismograms Using the S Transform. *Bull. Seism. Soc. Am.* **99**:**1**, 226–234.

Pinnegar, C. R., and D. E. Eaton (2003). Application of the S-transform to prestack noise attenuation filtering. *J. Geophys. Res.* , **108**:**B9**, 2422, doi 10.1029/2002JB00002258.

Stockwell, R. G., L. Mansinha, and R. P. Lowe (1996). Localization of the complex spectrum: the S transform.

IEEE Trans. Signal Process. **44**, 998–1001.
Tichelarr, B.W. and Ruff, L.J. (1989) How good are our best models? Jackknifing, Bootstraping, and Earthquake Depth. *EOS* **70: 593**,606-606, 1989.
Tokimatsu, K. (1997) Geotechnical site characterization using surface waves. *1st Intl. Conf. Earthquake Geotechnical Engineering*.
Wessel, P., and W.H.F. Smith (1991) Free software helps map and display data. *EOS Trans. AGU,* **72***,* 441.
Woolery, E. W., and R. Street (2002) 3D near-surface soil response from H/V ambient-noise ratios. *Soil Dyn. Earth. Eng.* **22***,* 865-876.